Journal of Solid State Chemistry **167,** 152–159 (2002)
doi:10.1006/jssc.2002.9637

Synthesis and Thermal Decomposition of Mn–Al Layered Double Hydroxides

Sumio Aisawa, Hidetoshi Hirahara, Hiroaki Uchiyama, Satoshi Takahashi, and Eiichi Narita[1]

Department of Chemical Engineering, Faculty of Engineering, Iwate University, 4-3-5 Ueda, Morioka, Iwate 020-8551, Japan

Received January 2, 2002; in revised form April 26, 2002; accepted May 3, 2002

In this paper, the synthesis and thermal decomposition behavior of hydrotalcite-like Mn–Al layered double hydroxide (LDH) have been investigated. First, the Mn–Al LDH was synthesized by the coprecipitation method using various anions such as Cl^-, CO_3^{2-}, NO_3^-, SO_4^{2-} or dicarboxylic acids (DCA). The single phase of the Mn–Al LDH was obtained when Cl^-, NO_3^- or DCA was used as a guest anion. In the case of CO_3^{2-} or SO_4^{2-}, the solid products included $MnCO_3$ or shigaite as a by-product. The crystallinity of the Cl/Mn–Al LDH was greatly influenced by a drying temperature and that the crystallinity of the Cl/Mn–Al LDH dried at room temperature was found to rise about 6 times in comparison with that dried at 333 K. The DCA/Mn–Al LDH was found to have an expanding LDH structure, supporting that the LDH basal layers were bridged by the intercalated DCA anion. Then, the thermal decomposition of the DCA/Mn–Al LDH has been examined, and the intercalated DCA was found to be decomposed at lower temperature than DCA itself. The oxidation number of Mn ion rose with increasing the heat treatment temperature and was +2.70 with crystallizing Mn_3O_4 after being heated at 973 K. The thermal decomposition of guest DCA was thought to be accelerated by the strong catalytic action of Mn ion in the host hydroxide basal layers. © 2002 Elsevier Science (USA)

Key Words: **Mn–Al layered double hydroxide; intercalation; coprecipitation; dicarboxylic acid; thermal decomposition; catalytic action.**

INTRODUCTION

Layered double hydroxide (LDH) is well known as hydrotalcite-like compounds or anionic clay because of its anion exchange property (1–3). In particular, the CO_3/Mg–Al LDH is one of the most frequently studied LDHs and is found in nature as hydrotalcite. LDH has been receiving increasing attention in recent years, owing to its potential technological applications such as catalysis, electrode, optical memory, separator, adsorbent, precursor for composite materials, and ion exchanger (4–8). The general formula of LDH is $[M^{2+}_{1-x}M^{3+}_x(OH)_2]^{X+}[A^{n-}_{X/n}\bullet yH_2O]^{X-}$, where M^{2+} is a divalent cation such as Mg^{2+}, Zn^{2+}, Co^{2+}, Ca^{2+}, Cu^{2+}, etc., M^{3+} a trivalent cation such as Al^{3+}, Cr^{3+}, Fe^{3+}, Co^{3+}, Mn^{3+}, etc., A^{n-} an anion of charge (n–) such as OH^-, Cl^-, NO_3^-, CO_3^{2-}, SO_4^{2-}, etc. LDH has a positively charged hydroxide basal layer due to the trivalent cation substituted for the divalent cation in the hydroxide basal layer and is electrically balanced by the intercalation of anion with water molecules into the interlayer space.

Recently, the synthesis of the novel organic/inorganic hybrid materials has great attractions. LDH is often used as an inorganic host material to synthesize the organic/LDH hybrid material (9–14). As the molecular arrangement in hybrid material can be regulated by nanoscale level, it has the possibility to show the characteristic of not possessing in each organic substance or inorganic substance. From a viewpoint of the addition of new function and organic modification of LDH, the synthesis of organic/LDH composites has been studied by means of intercalation technique of organic substances into LDH.

On the other hand, the use of the combination of various divalent and trivalent metal ions was reported for the synthesis of new M^{2+}–M^{3+} LDHs (15–22). However, Mn^{2+} was hardly used as the component of LDH basal layer. Only Malherbe *et al.* have reported the synthesis of the Cl/Mn–Al LDH (23), and there are few reports on the synthesis of the M^{2+}–Mn^{3+} LDH. The synthesis and thermal decomposition of the CO_3/Mg–Mn LDH was reported (24). The Ni–Mn LDH was synthesized, in which the added Mn^{2+} was oxidized to Mn^{3+} under alkaline condition during the synthesis of LDH (25). For applying as an electron transfer media, the electrochemical activity of the modified electrode with the CO_3/Mg–Mn LDH has also been investigated (26).

From a viewpoint of removal of pollutant, dicarboxylic acids (DCA) is often needed to remove from an industrial

[1]To whom correspondence should be addressed. Fax: +81-19-621-6331. E-mail: enarita@iwate-u.ac.jp.

0022-4596/02 $35.00

wastewater because DCA is widely used as a raw material of polyester and a hardener of phenol resin. The aim of the present paper is to investigate the synthesis of hydrotalcite-like Mn–Al LDH, and the intercalation of various DCA into the Mn–Al LDH by the coprecipitation method. The intercalation of DCA for LDH and the thermal decomposition of DCA/M^{2+}–M^{3+} LDH have been reported (27–29), because DCA is divalent anion in solution and easily intercalated for LDH. We have also investigated the thermal decomposition of DCA in the Mn–Al LDH.

EXPERIMENTAL

Materials

DCA and other inorganic reagents were purchased from Wako Pure Chemical Industries, Ltd., Japan.

Synthesis of Mn–Al LDH by Coprecipitation

The Mn–Al LDH precipitate was prepared by the standard aqueous coprecipitation method. A mixed solution of 1 M $Mn(NO_3)_2$ and $Al(NO_3)_3$ (Mn^{2+}/Al molar ratio = 2/1) was added dropwise to 1 M guest inorganic anion solution (NaCl, Na_2CO_3, $NaNO_3$ or Na_2SO_4) with stirring under a nitrogen atmosphere. Solution pH was adjusted to 9 by dropwise addition of 1 M NaOH solution, and temperature was kept at 313 K in a thermostat set. The resulting precipitate was aged for 1 h in the mother liquor and then collected by centrifugation. The solid product was washed with distilled water several times and dried in vacuum desiccator or vacuum oven for 24 h. Unless otherwise noted, the drying temperature was a room temperature.

Synthesis of DCA/Mn–Al LDH by Coprecipitation

The mixed solution of 1 M $Mn(NO_3)_2$ and $Al(NO_3)_3$ (Mn^{2+}/Al^{3+}/DCA molar ratio = 2/1/1) was added dropwise to 0.025 M DCA solution (succinic acid: Suc, adipic acid: Adi, suberic acid: Sub, sebacic acid: Seb, and dodecandionic acid: Dod) with stirring under a nitrogen atmosphere. Solution pH was adjusted to 9 by dropwise addition of 1 M NaOH solution, and temperature was kept at 313 K in a thermostat set. The resulting precipitate was aged for 1 h in the mother liquor and then collected by centrifugation. The supernatant solution was subjected for the measurement of DCA concentration by using Shimadzu TOC-5000 total organic carbon analyzer. The solid product was washed with distilled water several times and dried in the vacuum desiccator at room temperature for 24 h.

Heat Treatment of DCA/Mn–Al LDH

The heat treatment of the DCA/Mn–Al LDH was carried out using an ULVAC infrared image furnace HPC-7000. All samples were heated in air at a rate of 10 K/min and kept at a desired temperature for 90 min.

Characterization

Powder X-ray diffraction (XRD) patterns were recorded on a Rigaku Rint 2200 powder X-ray diffractometer, using a Cu$K\alpha$ ($\lambda = 0.15405$ nm) radiation with Ni filtered at 20 mA and 40 kV, 2θ angle ranged from 2–70° and a scanning rate of 2°/min. Fourier transform–infrared (FT–IR) spectra of KBr disks were recorded on a JASCO WS/IR 7300 FT–IR spectrophotometer. Thermogravimetry (TG) and differential thermal analysis (DTA) curves were recorded on a Seiko TG/DTA 320. All samples were heated in air at a rate of 10 K/min in the temperature range 298–1073 K. Chemical analysis data of the solid product was determined using a Hitachi 180-80 atomic adsorption spectrometer (metal ion), TOA Electronics IA-100 ion analyzer (nitrate ion) and Shimadzu TOC-5000 total organic carbon analyzer (DCA), respectively. Scanning electron micrographs (SEM) were performed using a Hitachi S-2250 scanning electron microscope. The oxidation number of Mn ion was determined by using a redox titration with oxalic acid and $KMnO_4$.

RESULTS AND DISCUSSION

Synthesis of Mn–Al LDH

The synthesis of the Mn–Al LDH incorporating various inorganic anions has been investigated by the coprecipitation method using Cl^-, CO_3^{2-}, NO_3^- or SO_4^{2-} as a guest anion. The XRD patterns and chemical compositions of the solid products are shown in Fig. 1 and Table 1, respectively. In the case of using Cl^- as a guest anion, the main diffraction peaks ($d_{003} = 0.78$ nm and $d_{006} = 0.39$ nm) were observed in Fig. 1(a), indicating LDH structure. As compared with the general Cl/M^{2+}–M^{3+} LDHs (for instance, Mg–Al and Zn–Al LDHs), the crystallinity of the Cl/Mn–Al LDH was lower than that of the Cl/M^{2+}–M^{3+} LDHs. The chemical composition of the Cl/Mn–Al LDH indicates that the molar ratio Mn^{2+}/Al^{3+}/Cl^- agreed with the stoichiometry of LDH. Therefore, the well-crystallized Cl/Mn–Al LDH can be synthesized by the standard coprecipitation method.

When CO_3^{2-} was used as a guest anion, the main diffraction peaks of the solid product corresponded to the general CO_3/M^{2+}–M^{3+} LDHs ($d_{003} = 0.76$ nm and $d_{006} = 0.38$ nm) as shown in Fig. 1(b), although the diffraction peaks of $MnCO_3$ (30) were also observed. The amount of CO_3^{2-} contained (molar ratio CO_3^{2-}/Al^{3+} = 1.31) in the

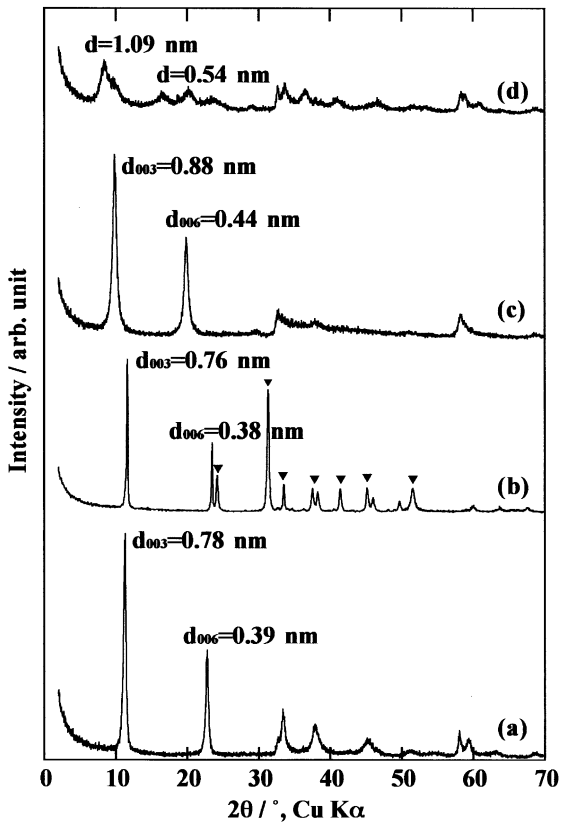

FIG. 1. XRD patterns of solid products. Guest anion: (a) Cl^-, (b) CO_3^{2-}, (c) NO_3^-, and (d) SO_4^{2-}. ▼: $MnCO_3$.

solid product disagreed with the stoichiometry of LDH, indicating that the solid product contained $MnCO_3$ as a by-product. Some CO_3/M^{2+}–M^{3+} LDHs generally have the ability of the calcination–rehydration reaction. However, the CO_3/Mn–Al LDH did not have it because it changed to a stable Mn oxide (e.g., Mn_3O_4) with calcination.

In the case of using NO_3^- as a guest anion, the intensive diffraction peaks ($d_{003} = 0.88$ nm and $d_{006} = 0.44$ nm) were observed with LDH structure in Fig. 1(c). The molar ratio $Mn^{2+}/Al^{3+}/NO_3^-$ was 1.95/1.00/0.99 and agreed with the stoichiometry of LDH. This result indicates that the single phase of the NO_3/Mn–Al LDH can be synthesized by the coprecipitation method.

When SO_4^{2-} was used as a guest ion, the crystallinity of the solid product was quite lower than that of the other inorganic anion/Mn–Al LDHs. Broad diffraction peaks ($d = 1.09$ and 0.54 nm) were observed without the LDH structure, which corresponded to shigaite ($Al_4Mn_7(SO_4)_2(OH)_{22}\cdot 8H_2O$) (31). The molar ratio Mn^{2+}/Al^{3+} of the solid product conforms to that of the initial combined source; however, the amounts of NO_3^- and SO_4^{2-} intercalated was inconsistent with the stoichiometry of LDH (molar ratio NO_3^- and $SO_4^{2-}/Al^3 = 1.24$). Thus, the single phase of the SO_4/Mn–Al LDH was difficult to synthesize by coprecipitation method.

These results indicate that the single phase of the inorganic anion/Mn–Al LDH was obtained when Cl^- or NO_3^- was used as a guest anion.

TABLE 1
Chemical Compositions of Various Mn–Al LDHs

Chemical composition of inorganic anion/Mn–Al LDH	Molar ratio Mn^{2+}/Al^{3+}	Molar ratio A^{n-}/Al^{3+}
$[Mn_{0.665}Al_{0.335}(OH)_2][Cl_{0.341}\cdot 0.513H_2O]$	1.99	1.01
$[Mn_{0.653}Al_{0.347}(OH)_2][(CO_3)_{0.227}\cdot 0.502H_2O]$	2.11	1.31
$[Mn_{0.671}Al_{0.329}(OH)_2][(NO_3)_{0.332}\cdot 0.499H_2O]$	1.95	1.00
$[Mn_{0.651}Al_{0.349}(OH)_2][(SO_4)_{0.156}(NO_3)_{0.121}\cdot 0.531H_2O]$	1.87	1.24
Chemical composition of DCA/Mn–Al LDH	**Mn^{2+}/Al^{3+}**	**DCA/Al^{3+}**
$[Mn_{0.662}Al_{0.338}(OH)_2][Suc_{0.168}(NO_3)_{0.002}\cdot 0.630H_2O]$	1.96	0.49
$[Mn_{0.671}Al_{0.329}(OH)_2][Adi_{0.163}(NO_3)_{0.003}\cdot 0.594H_2O]$	2.03	0.49
$[Mn_{0.655}Al_{0.345}(OH)_2][Sub_{0.169}(NO_3)_{0.007}\cdot 0.571H_2O]$	1.90	0.49
$[Mn_{0.680}Al_{0.320}(OH)_2][Seb_{0.150}(NO_3)_{0.020}\cdot 0.559H_2O]$	2.13	0.47
$[Mn_{0.662}Al_{0.338}(OH)_2][Dod_{0.154}(NO_3)_{0.026}\cdot 0.554H_2O]$	1.96	0.46

Influence of Drying Temperature on Crystallinity of Mn–Al LDH

It is possible that Mn^{2+} in the LDH basal layer is oxidized during synthesis, washing or drying procedure. In this section, the influence of a drying temperature on the crystallinity of the Cl/Mn–Al LDH has been investigated. The XRD patterns of the Cl/Mn–Al LDHs dried at room temperature, 313, and 333 K are shown in Fig. 2. All the Cl/Mn–Al LDHs indicate LDH structure ($d_{003} = 0.78$ nm and $d_{006} = 0.39$ nm); however, the crystallinity of Cl/Mn–Al LDH was quite different and decreased with increasing the drying temperature. As compared with the crystallinity of the Cl/Mn–Al LDH dried at room temperature and 333 K, the crystallinity of the former was about 6 times higher than that of the latter. Then, the oxidation number of Mn ion in the Cl/Mn–Al LDH was also examined. The oxidation number of Mn ion in the Cl/Mn–Al LDH slurry obtained just after precipitation was found to be +2.00; however, that in the Cl/Mn–Al LDH dried at 333 K increased to +2.13. The color of the Cl/Mn–Al LDH changed from white to light yellow with an increase in the drying temperature. This phenomenon has not been observed in the classical LDHs, suggesting that a thermal stability of the Mn–Al LDH is quite lower than the classical LDHs. These results indicate that Mn^{2+} on the surface of the LDH basal layer was slightly oxidized by oxygen in air during washing and/or drying procedure.

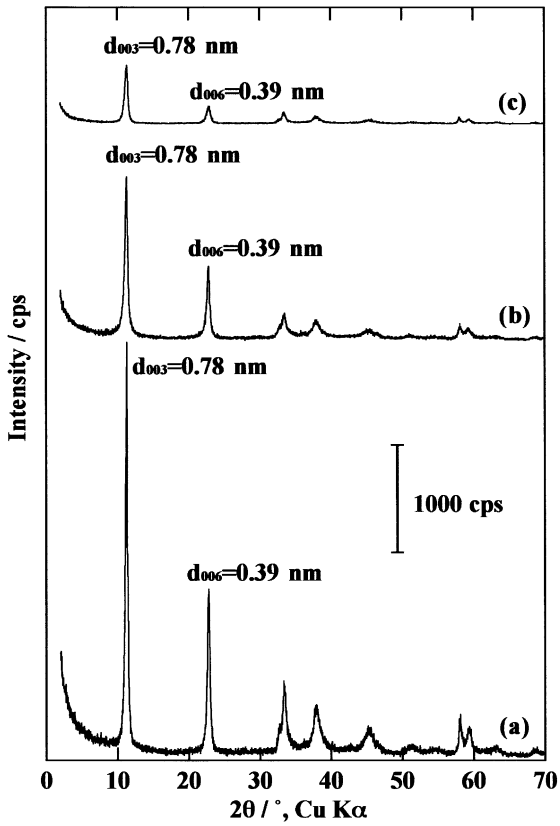

FIG. 2. XRD patterns of Cl/Mn–Al LDH dried at (a) room temperature, (b) 313 K, and (c) 333 K.

Moreover, the increase in the oxidation number of Mn ion was also found in the other inorganic anion/Mn–Al LDHs.

From the results, the crystallinity of the Mn–Al LDH was found to be remarkably influenced by the drying temperature. The resulting solid product should be dried at low temperature without air atmosphere in order to obtain the well-crystallized single phase of the Mn–Al LDH.

Synthesis of DCA/Mn–Al LDH

In this section, the synthesis of the DCA/Mn–Al LDH using Suc, Adi, Sub, Seb and Dod as a guest anion has been investigated. Table 1 indicates the chemical composition of the resulting solid products. As the anion exchange capacity of LDH is theoretically 1.00 mol/mol of Al for monovalent anion, it should be 0.50 mol/mol of Al for DCA because DCA exists as divalent cation in aqueous solution. The molar ratios of the solid products are almost agreed with the stoichiometry of LDH as follows: $Mn^{2+}/Al^{3+} = 1.90$–2.13 and $DCA/Al^{3+} = 0.46$–0.49. NO_3^- was slightly co-intercalated for the supplement of an excessive electric charge of the LDH basal layer. The amount of NO_3^- co-intercalated was increased with increasing the methylene chain length of DCA. The Mn^{2+} in the LDH basal layer is possible to be oxidized to Mn^{3+} or Mn^{4+} during the formation process of the LDH. However, the total amount of intercalated anion agreed with the stoichiometry of LDH, namely, the molar ratio $Mn^{2+}/Al^{3+}/$(DCA and NO_3^-) was 2/1/1. This result indicates that Mn^{2+} in the basal layer was hardly oxidized during the formation process of the LDH.

The XRD patterns of the solid products are shown in Fig. 3. The solid products possess LDH structure with low crystallinity. The basal spacing, d_{003}, of the DCA/Mn–Al LDH was 1.19 (Suc), 1.30 (Adi), 1.47 (Sub), 1.61 (Seb), and 1.73 (Dod) nm and increased linearly with an increase in the methylene chain length of DCA as shown in Fig. 3 inset. These results corresponded to that of the previous report (27), in which Miyata and Kumura indicated that the expanded basal spacing of the DCA/Mn–Al LDH was proportional to the carbon number of DCA. As the

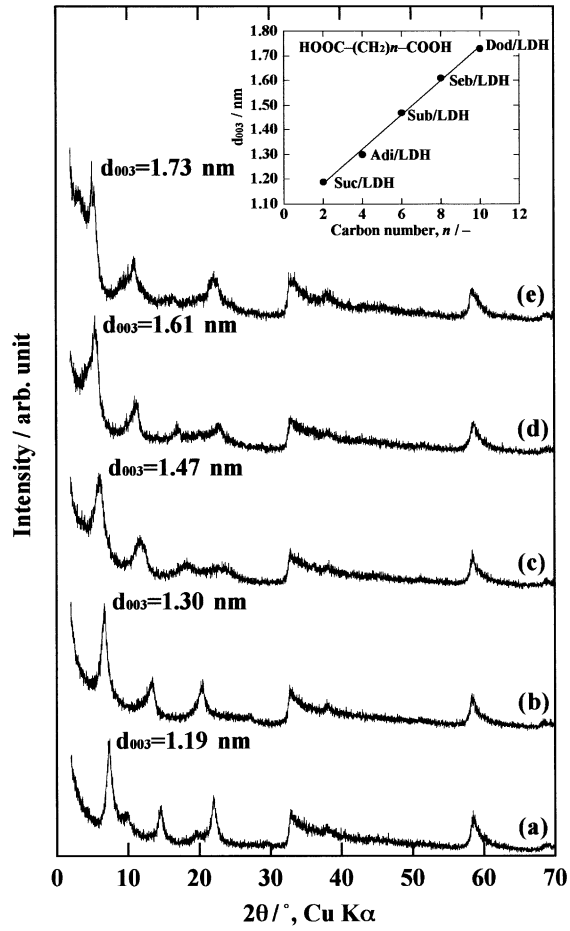

FIG. 3. XRD patterns of solid products. Guest anion: (a) Suc, (b) Adi, (c) Sub, (d) Seb, and (e) Dod. Inset: relationship between basal spacing of solid products and carbon number of guest DCA.

thickness of LDH basal layer is 0.48 nm, the interlayer space of the DCA/Mn–Al LDH was estimated as 0.71, 0.82, 0.99, 1.13, and 1.25 nm, respectively. The expansion of the interlayer space indicates that DCA makes the bridged LDH basal layer structure. The FT–IR spectra of the DCA/Mn–Al LDH are shown in Fig. 4. Broad absorption peaks in the region 2800–3600 and 1560 cm^{-1} are assigned to O–H group stretches and deformation vibration of the hydroxides basal layer or interlayer water molecule. The lattice vibration modes are observed by M–O (550, 590, and 840 cm^{-1}) and O–M–O (430 cm^{-1}) vibrations. The absorption peaks of alkyl C–H antisymmetric, symmetric stretch, and deformation vibration were observed at 1400, 2850, and 2925 cm^{-1}, respectively. In particular, the alkyl C–H stretch absorption was increased with an increase in the methylene chain length of the intercalated DCA. The strong absorption peak of COO^- antisymmetric vibration was shown at 1580 cm^{-1}. The SEM images of the Seb/Mn–Al LDH are shown in Fig. 5. In general, LDH crystal has plate-like morphology and hexagonal crystallite. Although the part of the LDH is coagulated, the Seb/Mn–Al LDH has only the plate-like morphology and the hexagonal crystallite.

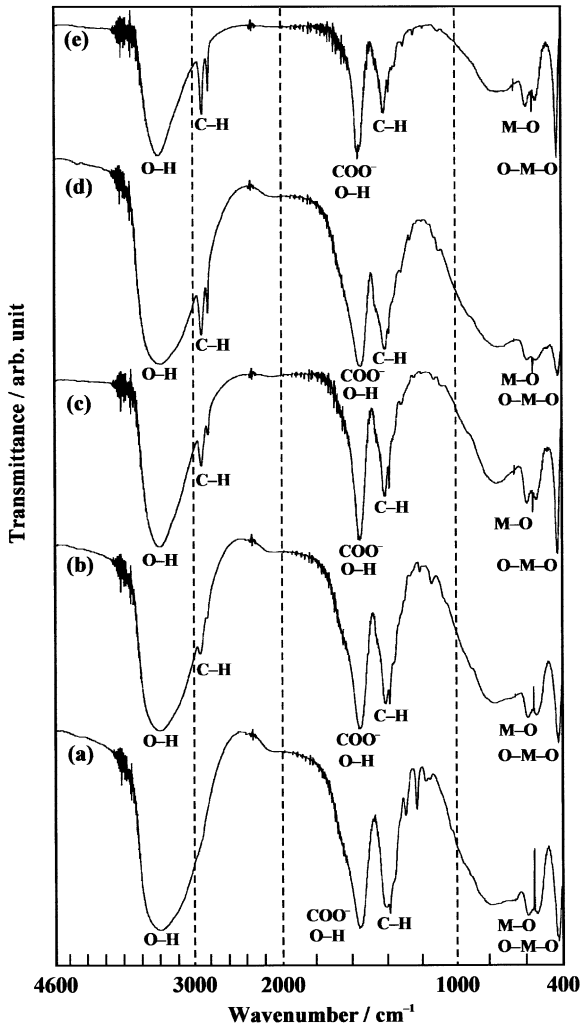

FIG. 4. FT–IR spectra of (a) Suc/Mn–Al LDH, (b) Adi/Mn–Al LDH, (c) Sub/Mn–Al LDH, (d) Seb/Mn–Al LDH, and (e) Dod/Mn–Al LDH.

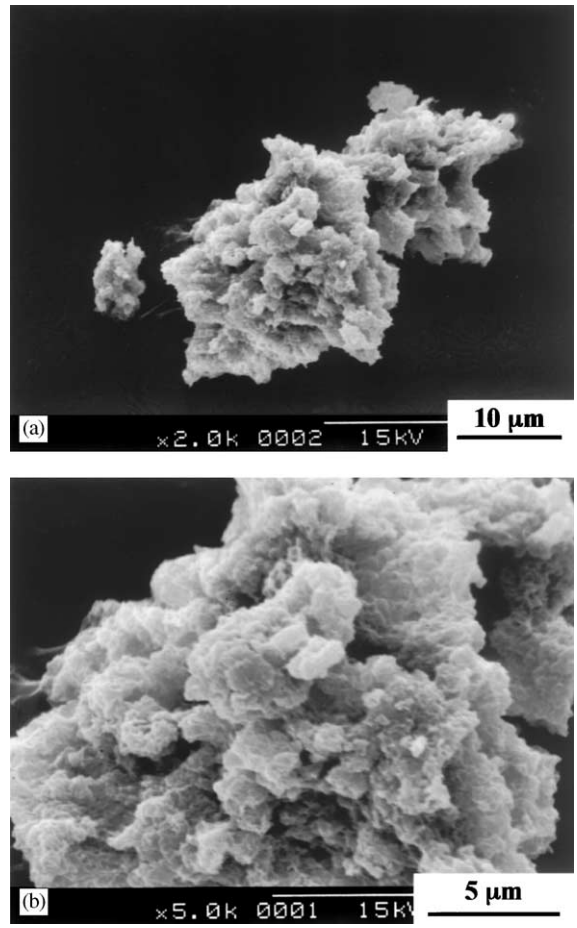

FIG. 5. SEM images of Seb/Mn–Al LDH. Magnification: (a) 2 k and (b) 5 k.

Schematic models of the Dod and Suc/Mn–Al LDH are depicted in Fig. 6. As DCA completely dissociated in the aqueous solution at pH 9 and existed as divalent anion, it was thought that the intercalated DCA was oriented vertically for the LDH basal layer with crosslinking between the LDH basal layers by α, ω-carboxylate groups. However, the expansion of interlayer spacing was disagreed with the molecular length of DCA (Sub, Seb, and Dod), indicating that they are obliquely oriented with a slanting angle of ca. 60° for the LDH basal layer (28). The small amount of NO_3^- co-intercalated in the Seb and Dod/Mn–Al LDHs was larger than that of other DCA/Mn–Al LDHs as shown in Table 1. Therefore, the non-absorption site was thought to be occupied by NO_3^- with keeping the electric balance of the LDH.

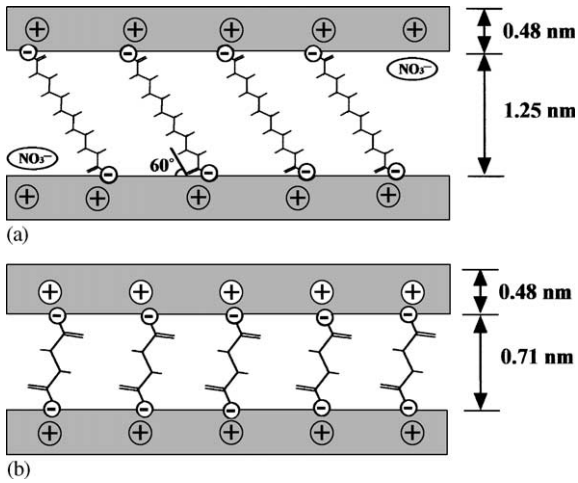

FIG. 6. Schematic illustrations of (a) Dod/Mn–Al LDH and (b) Suc/Mn–Al LDH.

Thermal Decomposition of DCA/Mn–Al LDH

In this section, the thermal decomposition behavior of the DCA/Mn–Al LDH has been studied. The TG–DTA curves of the DCA/Mn–Al LDH are shown in Fig. 7. Total weight loss of the DCA/Mn–Al LDH was ca. 40–50%. The gentle weight losses by removal of the adsorbed water, interlayer water, and the dehydroxylation of the LDH basal layer were observed for all the DCA/Mn–Al LDHs in the temperature region 300–500 K. The rapid weight losses and exothermic peaks by the decomposition and combustion of the intercalated DCA were also observed in the temperature region 500–600 K. In the case of the Suc and Dod/Mn–Al LDHs, the combustion of the intercalated DCA occurred by one step, namely, the intercalated Suc and Dod was decomposed via the formation of acid anhydride by the dehydration of carboxyl groups. On the other hand, the two steps weight losses and the combustion of the intercalated Adi, Sub, and Seb was observed at 543 K and in the temperature region 595–612 K. It means that the intercalated Adi, Sub, and Seb was decomposed to the monocarboxylic acids with the heat treatment; therefore, the two exothermic peaks were observed. These results indicated that the decomposition temperature of DCA became lower by the intercalation into the Mn–Al LDH. The decomposition of the intercalated organic substance was accelerated by the catalytic action of Mn ion in the LDH basal layer. In general, in LDH systems such as the Mg–Al and Zn–Al LDH such phenomenon did not occur, and this is the most interesting feature of the Mn–Al LDH.

The change in the crystal structure of the Suc and Sub/Mn–Al LDH with the heat treatment has been studied. The XRD patterns of the solid products after the heat treatment are shown in Fig. 8. The Suc/Mn–Al LDH kept a layered structure at 378 K; however, the diffraction peak of (003) shifted to high angle (from 1.19 to 0.90 nm). Suc is thought to be vertically oriented for the LDH basal layer,

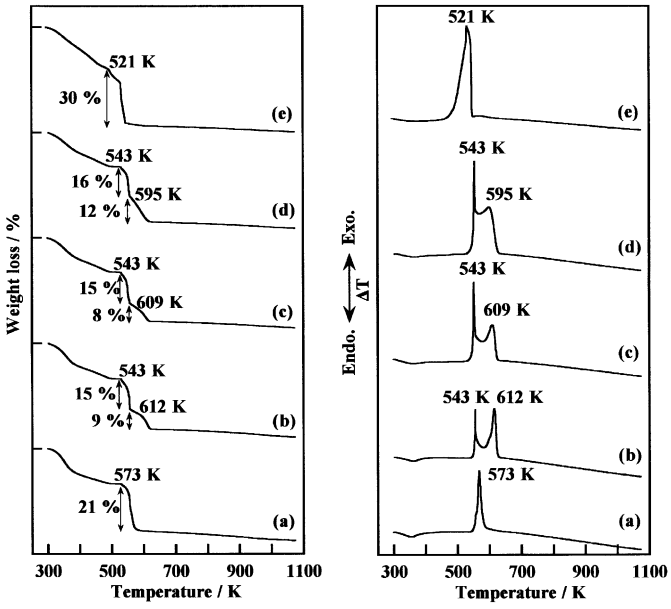

FIG. 7. TG–DTA curves of (a) Suc/Mn–Al LDH, (b) Adi/Mn–Al LDH, (c) Sub/Mn–Al LDH, (d) Seb/Mn–Al LDH, and (e) Dod/Mn–Al LDH.

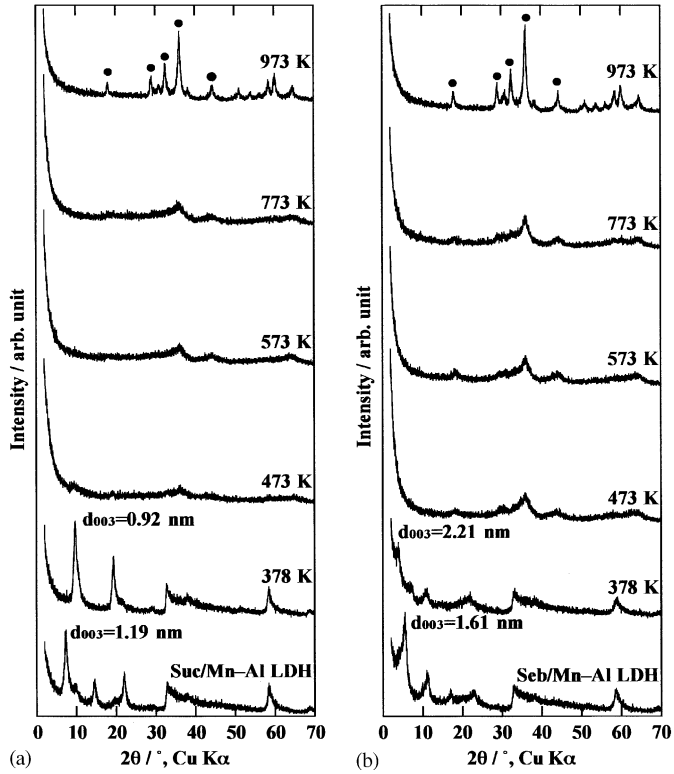

FIG. 8. XRD patterns of (a) Suc/Mn–Al LDH and (b) Seb/Mn–Al LDH obtained after heat treatment at various temperatures. ●: Mn_3O_4.

and the orientation of Suc is changed with the heat treatment, in which the orientation angle of Suc was estimated as ca. 50° for the LDH basal layer. This is because the stability of the intercalated DCA was influenced by the energy of interaction between the water molecule and the layered host structure (29). The reduction of basal layer was also observed in the Adi/Mn–Al LDH (from 1.30 to 0.94 nm) with the heat treatment. In the temperature range 473–773 K, the layered structure of the Sub/Mn–Al LDH was completely destroyed, and then the solid product crystallized to Mn_3O_4 (hausmannite) (32) at 973 K. On the other hand, the Sub/Mn–Al LDH kept the LDH structure still at 378 K. The diffraction peak of (003) was shifted to low angle (from 1.16 to 2.21 nm) with decreasing the crystallinity. The intercalated Sub was first slantingly orientated with an angle of ca. 60° for the basal layer, suggesting that the orientation of Sub was changed to the vertical orientation by the heat treatment. It was presumed that the interaction of host–host or host–guest was diminished by the dehydration of interlayer water such as the electrostatic force and hydrogen bonding. Therefore, the intercalated DCA was able to move in the LDH interlayer space, the orientation of DCA being changed to the vertical orientation for the LDH basal layer. The expanding basal layer with the heat treatment was also observed in the Seb/Mn–Al LDH (from 1.16 to 2.36 nm) and Dod/Mn–Al LDH (from 1.73 to 2.94 nm). The basal spacing of the Sub, Seb, and Dod/Mn–Al LDH with the heat treatment at 378 K was increased with increase in the methylene chain length of DCA. When the Sub/Mn–Al LDH was heated at 973 K, the solid product also crystallized to Mn_3O_4 is the same way as the Suc/Mn–Al LDH.

The temperature dependence of the oxidation number of Mn ion in the LDH basal layer is shown in Fig. 9. The rise of oxidation number of Mn ion (max. +2.20) was observed at 298 K, suggesting that a part of Mn^{2+} in the basal layer was oxidized by air although the solid product was dried at room temperature. In particular, the interlayer expansion is large such as the Seb and Dod/Mn–Al LDHs, which were easily influenced by the air oxidation. It was assumed that the specific surface area of the DCA/Mn–Al LDH may be increased with expanding interlayer space; therefore, the Mn–Al LDH was oxidized by oxygen in air with increase in contact of surface area. The oxidation number of Mn ion was increased to +2.10–2.30 at 378 K, and the rapid rise of the oxidation number was observed in the temperature range 473–573 K. This temperature range is agreed with decomposition and combustion of the intercalated DCA as shown in DTA curves (Fig. 7). It means that the oxidation number was influenced by the combustion of the intercalated DCA, and it became maximum at +2.90–3.20 at 573 K. However, the oxidation number of Mn ion was decreased with increasing temperature and gradually diminished to +2.70 because the theoretical oxidation number of Mn ion in Mn_3O_4 is +2.70. When the Suc and Seb/Mn–Al LDH were heated at 973 K, the solid products crystallized to Mn_3O_4 as shown in Fig. 8. In the case of the other DCA/Mn–Al LDH, the formation of Mn_3O_4 was confirmed by the heat treatment. As a result, the oxidation number of Mn ion in the LDH basal layer was greatly influenced by the decomposition and combustion of the intercalated DCA.

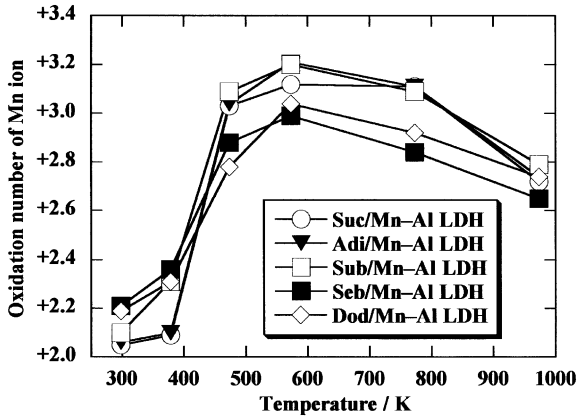

FIG. 9. Temperature dependence of oxidation number of Mn ion in host layer.

CONCLUSION

The Mn–Al LDH was successfully synthesized by the coprecipitation method. The single phase of the inorganic anion/Mn–Al LDH was obtained when Cl^- or NO_3^- is used as a guest anion. In the presence of CO_3^{2-} or SO_4^{2-}, the solid products included $MnCO_3$ or shigaite as a by-product. The crystallinity of the Mn–Al LDH was influenced by a drying temperature, in which a part of Mn^{2+} in the LDH basal layer was oxidized during drying. When the Mn–Al LDH was dried at room temperature, the well-crystallined Mn–Al LDH was obtained. The DCA/Mn–Al LDH was also synthesized by the coprecipitation method. The orientation change of intercalated DCA with the heat treatment was influenced by the length of DCA, and the decomposition temperature of the intercalated DCA was found to be lower than DCA itself. It indicates that the Mn–Al LDH has a strong catalytic action for the decomposition of intercalated guest organic substances. These features of the Mn–Al LDH will be useful for the removal and catalytic decomposition of harmful organic anions.

REFERENCES

1. L. Ingram and H. F. W. Taylor, *Miner. Mag.* **36,** 465 (1967).
2. R. Allmann, *Acta Crystallogr., Sect. B* **24,** 972 (1968).

3. S. Miyata, *Clays Clay Miner*. **23,** 369 (1975).
4. B. Sels, D. De Vos, M. Buntinx, F. Pierard, A. K. Mesmaeker, and P. Jacobs, *Nature* **400,** 855 (1999).
5. H. Sakaebe, H. Uchino, M. Azuma M. Shikano, and S. Higuchi, *Solid State Ionics* **113–115,** 35 (1998).
6. T. Kuwahara, H. Tagaya, J. Kadokawa, and K. Chiba, *J. Mater. Synth. Proc*. **4,** 69 (1996).
7. A. M. Fogg, V. M. Green, H. G. Harvey, and D. O'Hare, *Adv. Mater*. **11,** 1466 (1999).
8. Y. Seida and Y. Nakano, *Water Res*. **34,** 1487 (2000).
9. S. P. Newman and W. Jones, *New J. Chem*. **22,** 105 (1998).
10. J. Choy, S. Kwak, J. Park, Y. Jeong, and J. Portier, *J. Am. Chem. Soc*. **121,** 1399 (1999).
11. M. Lakraimi, A. Legrouri, A. Barroug, A. De Roy, and J. P. Besse, *J. Mater. Chem*. **10,** 1007 (2000).
12. M. Ogawa and S. Asai, *Chem. Mater*. **12,** 3253 (2000).
13. J. Choy, S. Kwak, J. Park, and Y. Jeong, *J. Mater. Chem*. **11,** 1671 (2001).
14. S. Aisawa, S. Takahashi, W. Ogasawara, Y. Umetsu, and E. Narita, *J. Solid States Chem*. **162,** 52 (2001).
15. F. M. Vichi and O. L. Alves, *J. Mater. Chem*. **7,** 1631 (1997).
16. M. R. Weir and R. A. Kydd, *Inorg. Chem*. **37,** 5619 (1998).
17. M. Del Arco, P. Malet, R. Trujillano, and V. Rives, *Chem. Mater*. **11,** 624 (1999).
18. F. M. Labajos, M. D. Sastre, R. Trujillano, and V. Rives, *J. Mater. Chem*. **9,** 1033 (1999).
19. M. Á. Aramendía, V. Borau, C. Jiménez, J. M. Marinas, F. J. Romero, and F. J. Urbano, *J. Mater. Chem*. **9,** 2291 (1999).
20. Z. P. Xu and H. C. Zeng, *Chem. Mater*. **12,** 2597 (2000).
21. S. Kannan and R. V. Jasra, *J. Mater. Chem*. **10,** 2311 (2000).
22. W. Hou, Y. Su, D. Sun, and C. Zhang, *Langmuir* **17,** 1885 (2001).
23. F. Malherbe, C. Forano, and J. P. Besse, *J. Mater. Sci. Lett*. **18,** 1217 (1999).
24. J. M. Fernandez, C. Barriga, M. Ulibarri, F. M. Labajos, and V. Rives, *J. Mater. Chem*. **4,** 1117 (1994).
25. C. Barriga, J. M. Fernández, M. A. Ulibarri, F. M. Labajos, and V. Rives, *J. Solid State Chem*. **124,** 205 (1996).
26. J. Qiu and G. Villemure, *J. Electroanal. Chem*. **428,** 165 (1997).
27. S. Miyata and T. Kumura, *Chem. Lett*. 843 (1973).
28. M. Meyn, K. Beneke, and G. Lagaly, *Inorg. Chem*. **29,** 5201 (1990).
29. V. Prevot, C. Forano, and J. P. Besse, *Inorg. Chem*. **37,** 4293 (1998).
30. JCPDS-ICDD, PDF Database No. 44–1472 (1997).
31. JCPDS-ICDD, PDF Database No. 38–428 (1997).
32. JCPDS-ICDD, PDF Database No. 24–73 (1997).